Electron Paramagnetic Resonance of the Excited Triplet State of Metal-Free and Metal-Substituted Cytochrome *c*

P. J. Angiolillo and J. M. Vanderkooi
Johnson Research Foundation, Department of Biochemistry and Biophysics, School of Medicine, University of Pennsylvania, Philadelphia, PA 19104 USA

ABSTRACT The photoactivated metastable triplet states of the porphyrin (free-base, i.e., metal-free) zinc and tin derivatives of horse cytochrome *c* were investigated using electron paramagnetic resonance. Zero-field splitting parameters, line shape, and Jahn–Teller distortion in the temperature range 3.8–150 K are discussed in terms of porphyrin–protein interactions. The zero-field splitting parameters $|D|$ for the free-base, Zn and Sn derivatives are 465×10^{-4}, 342×10^{-4}, and 353×10^{-4} cm^{-1}, respectively, and are temperature invariant over the temperature ranges studied. An $|E|$ value at 4 K of 73×10^{-4} cm^{-1} was obtained for Zn cytochrome *c*, larger than any previously found for Zn porphyrin derivatives of hemeproteins, showing that the heme site of cytochrome *c* imposes an asymmetric field. Though the $|E|$ value for Zn cytochrome *c* is large, the geometry of the site appears quite constrained, as indicated by a spectral line shape showing a single species. Intersystem crossing occurred predominantly to the $|T_2\rangle$ zero-field spin sublevel. EPR line shape changes with respect to temperature of Zn cyt *c* are interpreted in terms of vibronic coupling, and a maximum Jahn–Teller crystal-field splitting of approximately 180 cm^{-1} is obtained. Sn cytochrome *c* in comparison with the Zn protein exhibits a photoactivated triplet line shape that is less well resolved in the *X–Y* region. The $|E|$ value is approximately 60×10^{-4} cm^{-1} at 4 K; its value rapidly tends toward zero with increasing temperature, from which a value for the Jahn–Teller crystal-field splitting of ≥ 40 cm^{-1} is estimated. In contrast to those for the metal cytochromes, the $|E|$ value for the free-base derivative was essentially zero at all temperatures studied. This finding is discussed as a consequence of an excited-state tautomerization process that occurs even at 4 K.

INTRODUCTION

Cytochromes *c*, single polypeptide chain heme-containing proteins, are key "players" in biological electron transport processes. All organisms utilizing photosynthesis or mitochondrial oxidative phosphorylation have *c*-type cytochromes (Pettigrew and Moore, 1987). In mammalian systems, it is the penultimate electron transfer protein, shuttling electrons between its reductase (ubiquinol-cyt *c* reductase) and cyt *c* oxidase. Cytochromes *c* are unusual in that not only is the prosthetic heme moiety attached by covalent coordination to the protein through axial ligation on the central metal but the heme side groups also have covalent bonds to the protein. In the case of mammalian systems these bonds arise through condensation of the two vinyl attachments with cysteine 14 and 17. This biological modification allows the iron in cytochromes *c* to be replaced without removal of the porphyrin, unlike in other hemeproteins such as myoglobin, hemoglobin, and *b*-type cytochromes, in which there is no covalent attachment to the protein other than through axial ligation.

Removing the iron or replacing it with other metals, such as zinc and tin, renders the porphyrin of cyt *c* fluorescent and phosphorescent, with emission lifetimes spanning approximately 6 orders of magnitude (10 ns to 20 ms, respectively, for fluorescence and phosphorescence). This modification has made it amenable to studies using high-resolution optical spectroscopy (Angiolillo et al., 1982; Logovinsky et al., 1993; Leeson et al., 1994; Friedrich et al., 1994) in attempts to uncover chromophore–protein interactions as manifested in the electronic and vibronic structure. The further employment of these closed-shell metal derivatives of hemeproteins as photoactivatable models for energy and electron transfer with its natural and cross-species redox partners has provided a powerful approach and continues to grow (Elias et al., 1988; Zang and Maki, 1990; Wallin et al., 1991; Casimiro et al., 1993; Horie et al., 1984; vander Est, 1993; Zhou and Kostic, 1993a,b; Meier et al., 1994). In particular, the excited triplet state of these derivatives has been implicated in some of the proposed excited-state transfer mechanisms.

Despite the interest in the properties and reactions of excited states of porphyrin proteins, information outlining the photophysics of the excited states, in particular the metastable triplet state, has been lacking. Furthermore, advantage has not been taken of the information that might be gleaned about porphyrin–protein interactions from looking specifically at the triplet state.

Zn cyt *c* and Sn cyt *c*, like the free-base porphyrin derivative of cyt *c* (H cyt *c*), are diamagnetic in the ground state ($S = 0$). With visible wavelength excitation into the first excited singlet manifold and subsequent intersystem crossing

Received for publication 16 November 1994 and in final form 6 March 1995.
Address reprint requests to Dr. Jane Vanderkooi, Department of Biochemistry and Biophysics, University of Pennsylvania, Philadelphia, Pennsylvania 19104-6089. Tel.: 215-898-8783; FAX: 215-573-2042; E-mail: Vanderkooi@mscf.med.upenn.edu.

Abbreviations used: cyt c, cytochrome c; H cyt c: metal free cyt c; Zn cyt c: Fe replaced by Zn; Sn cyt c: Fe replaced by Sn; EPR, electron paramagnetic resonance, ZFS, zero-field splitting; ISC, intersystem crossing; ODMR, optically detected magnetic resonance; JT, Jahn-Teller; PP, protoporphyrin IX dimethyl ester; MP, mesoporphyrin IX dimethyl ester.

0006-3495/95/06/2505/14 $2.00

(ISC), a metastable triplet state is formed. Because the triplet state has a net spin of unity ($S = 1$), it is amenable to study by electron paramagnetic resonance (EPR) and optically detected magnetic resonance (ODMR).

In this paper we look at the photoactivated triplet state of the free-base zinc(II) and tin(IV) derivatives of cyt *c* (horse), from the standpoint of assessing local geometry and the spin dynamics, as manifested in the line-shape and zero field splitting (ZFS) parameters. Also, through the temperature dependencies of the ZFSs, the validity of the vibronic coupling scheme, as it applies to proteins, is investigated.

PORPHYRIN TRIPLET PHOTOPHYSICS

EPR line shape

The magnetic resonance of the lowest triplet excited state in porphyrins is that of a correlated ($S = 1$) spin system (Weltner, 1983). The spin Hamiltonian is governed mainly by the Zeeman interaction and the dipolar spin–spin interaction of the two electrons in the triplet molecular orbital. The nuclear hyperfine couplings are rarely, if ever, seen in randomly oriented triplets in external field because of the large anisotropy. Within the molecular axis system, the total spin Hamiltonian describing the Zeeman interaction and the interaction between the two spins is

$$H_T = \beta_e \mathbf{H} \cdot \mathbf{g} \cdot \mathbf{S} + \mathbf{S} \cdot \mathbf{D} \cdot \mathbf{S}, \qquad (1)$$

where $\mathbf{H}$ is the applied magnetic field, S is the total spin, $\mathbf{g}$ is the g-value tensor, and $\mathbf{D}$ is the ZFS tensor. For most organic triplets, the g-tensor can be replaced with the value for the free electron, $g_e \simeq 2.0023$, as the orbital angular momentum is essentially quenched (Schlicter, 1991). In a molecular axis system chosen such that the zero-field tensor is diagonal, the Hamiltonian becomes

$$H_T = g_e \beta_e \mathbf{H} \cdot \mathbf{S} - X S_x^2 - Y S_y^2 - Z S_t^2, \qquad (2)$$

where X, Y, and Z are the eigenvalues of the spin–spin interaction matrix and S_i ($i = x, y, z$) are the total spin angular momenta projections along the principal axes in zero magnetic field. Inasmuch as the ZFS tensor is traceless, i.e., $X + Y + Z = 0$, the Hamiltonian can be recast by using two independent parameters, D and E, giving the familiar phenomenological spin Hamiltonian

$$H_T = g_e \beta_e \mathbf{H} \cdot \mathbf{S} + D\left(S_z^2 - \frac{1}{3}S^2\right) + E(S_x^2 - S_y^2). \qquad (3)$$

The ZFS parameter D is a "measure" of the electron spatial distribution of the triplet molecular orbital and E is a "measure" of distortion from tetragonal symmetry.

The line shape for randomly oriented triplets was previously described (Kottis and Lefebvre, 1963, 1964; Wasserman et al., 1964). For each case, where the applied magnetic field is aligned with a principal molecular axis, three transitions are possible among the triplet sublevels (Fig. 1). In the strong-field limit, the triplet spin eigenfunctions are quantized along the axis of the applied field and are adequately given by

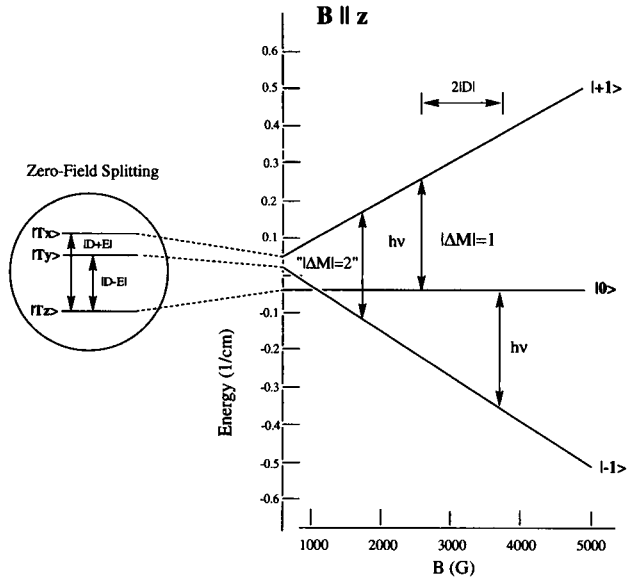

FIGURE 1 Energy diagram for the triplet-state spin components of the lowest triplet state of a metalloporphyrin as a function of applied magnetic field for one of the three canonical orientations ($H \parallel Z$). *X*-band frequency (~9 GHz) assumed. The exploded view to the left shows the hypothetical splitting of the triplet manifold in zero applied magnetic field in a rhombic environment. The assumptions are $D > 0$, $E > 0$.

$$|+1\rangle = |\alpha_1\alpha_2\rangle,$$

$$|0\rangle = 1/(2)^{1/2}(|\alpha_1\beta_2\rangle + |\beta_1\alpha_2\rangle),$$

$$|-1\rangle = |\beta_1\beta_2\rangle,$$

where $M = 1, 0, -1$ are the Z components of the spin angular momentum along the axis of quantization and $|\alpha\rangle$ and $\beta\rangle$ are the one electron spin eigenstates.

In zero applied field, the eigenfunctions have their spin quantized along the principal axes, which usually correspond to axes of symmetry. For porphyrins, as in other planar aromatic π–π^* systems, the z axis is taken as the out-of-plane axis with the x and y axes lying in plane normally along the axes of symmetry. The zero-field spin states, which diagonalize the ZFS tensor, are related to the strong-field eigenfunctions through the following transformation (Hameka and Oosterhoff, 1958):

$$|T_x\rangle = -(2^{-1/2})\,(|+1\rangle - |-1\rangle),$$

$$|T_y\rangle = i(2^{-1/2})\,(|+1\rangle + |-1\rangle),$$

$$|T_z\rangle = |0\rangle.$$

Thus, the eigenfunctions $|T_x\rangle$, $|T_y\rangle$, and $|T_z\rangle$ have energies X, Y, and Z, respectively, with the following conventional ordering $X > Y > Z$ (van der Waals et al., 1979).

Historically, the most prominent feature seen in the triplet EPR spectrum is an almost isotropic transition at $g \approx 4$, which corresponds to the pseudo $|\Delta M| = 2$ transition $|+1\rangle \leftrightarrow |-1\rangle$ (Fig. 1). Transitions in the $|\Delta M| = 1$ region,

$|0\rangle \leftrightarrow |+1\rangle$ and $|0\rangle \leftrightarrow |-1\rangle$, are symmetrically separated around $g_e = 2.0023$.

The anisotropy of the ZFSs, in general, leads to six observable lines or turning points in the first derivative spectrum in the $g_e = 2$ region, Z_l, Y_l, X_l, X_h, Y_h, and Z_h, going from low field to high field (Fig. 1). Assuming that D is positive, which is the usual assumption for flat planar aromatics, the $|0\rangle \leftrightarrow |+1\rangle$ transition has components at field positions displaced from the field position for a free electron ($h\nu/g_e\beta_e$) by $-D$, $+(D - 3E)/2$, and $+(D + 3E)/2$. Likewise, the $|0\rangle \leftrightarrow |-1\rangle$ transition has lines at field positions displaced from g_e by $+D$, $-(D - 3E)/2$, and $-(D + 3E)/2$, respectively. Thus, from the resulting "powder" spectrum, the ZFS parameters are readily extractable and are $\Delta H_z = 2|D|$, $\Delta H_y = |D + E|$, and $\Delta H_x = |D - E|$, where ΔH_i ($i = x, y, z$) are the separations of the pair of transitions (in Gauss).

Dynamic Jahn-Teller effect in a "crystal-field"

For square planar central metal porphyrins, the lowest triplet should be spatially degenerate and in the D_{4h} point group would have a representation of ^3E_u. The special characteristics of porphyrin-excited triplet states are reviewed by van der Waals et al. (1979). Because a porphyrin with C_4 or S_4 symmetry is JT unstable, it is subject to symmetry-relieving interactions resulting in two energy equivalent triplet states. JT instability alone is not enough to relieve the energy degeneracy of the triplet state, but interactions with axial ligands or porphyrin substituents or interaction with environmental asymmetries may stabilize one state with respect to the other by an energy of δ_{JT}. The resulting "powder" pattern EPR spectrum, when $\delta_{JT} \gg k_BT$, will show a static distortion with a nonzero $|E|$, with a splitting between the Y and X transitions (ΔH_{xy}) equal to $3|E|$. However, at temperatures that are comparable with or exceed the JT splitting energy, the X and Y transitions will merge, with complete coalescence occurring when both states are equally populated and when the exchange frequency, ν_{JT}, is greater than the separation of the X and Y transitions, i.e., when $\nu_{JT} \gg g_e\beta_e\Delta H_{xy}/h$ (Carrington and McLachlan, 1967). This temperature dependence of the X and Y transitions has been termed the dynamic Jahn-Teller effect.

One theory to account for the dynamic JT effect involves coupling to one of the in-plane porphyrin vibrational modes, giving rise to two vibronic triplets separated in energy by δ_{JT} (de Groot et al., 1969; van der Waals et al., 1979). The populations of the vibronic triplet states are governed by the Boltzmann distribution law and the in-plane anisotropy, as measured by the ZFS parameter $|E|$ will be temperature dependent. For square planar porphyrins of D_{4h} symmetry, coupling to either b_{1g} or b_{2g} vibrational modes has the effect of merely changing the sign of E, with $|E|$ unchanged. The distortions are equivalent to an interchange of the x and y molecular axes. The ramification is that, as $k_BT \gg \delta_{JT}$, the E value should approach zero and a coalescence of the Y and X transitions should occur. Thus, the in-plane anisotropy, as measured by the E ZFS parameter in Eq. 4, reduces to

$$E = E_0 \tanh\left(\frac{\delta_{JT}}{2k_BT}\right), \quad (4)$$

where E_0 is the value of E when $k_BT \gg \delta_{JT}$.

MATERIALS AND METHODS

Horse-heart cyt *c* (Type III) was purchased from Sigma Chemical Co. (St. Louis, MO). The free-base and metallo derivatives of cyt *c* were prepared by methods previously described (Vanderkooi et al., 1976; Vanderkooi and Erecinska, 1975). Protoporphyrin IX dimethyl ester (PP) and mesoporphyrin IX dimethyl ester (MP) were purchased from Porphyrin Products (Logan, UT) or Mid-Century (Posen, IL) and used without further purification. All solvents were spectral grade and degassed before use.

Instrumentation

EPR was performed on a Bruker ESP300E spectrometer. Intracavity illumination was performed directly through the front louvers with fiber optics using a 150-W Kuda quartz-halogen illuminator. Temperatures that ranged from 3.8 K upward were obtained by an Oxford ESR 900 continuous-flow cryostat controlled with an Oxford ITC4 temperature controller. Frequency was measured with a Hewlett-Packard 5350B microwave frequency counter. All experiments were conducted at microwave powers that ensured that there was no saturation of resonances. The spectra are presented as the resultants of light minus dark spectra; this procedure removed the contribution of a paramagnetic contamination present in the cavity. In most cases the irradiation procedure caused no permanent changes in the sample as monitored by absorption and emission spectra before and after intracavity irradiation. For Zn cyt *c*, in particular, prolonged irradiation at the highest temperatures led to the appearance of increased free-radical intensity, which allowed for internal field calibration.

Phosphorescence lifetimes were measured with the instrument described by Vanderkooi et al. (1987). Lifetimes were measured at 77 K in the same glassy matrices used for EPR with excitation at the Soret maximum and emission measured at the maximum of the (0–0) of the phosphorescence spectrum. Lifetimes were determined from decay profiles by analysis with the ASYSTANT program (Macmillan Software Co., New York, NY).

RESULTS

EPR spectra of Zn, Sn, and H cyt *c*

The EPR spectra of the photoactivated triplet state of Zn, Sn, and H cyt *c* at 4 K are given in Fig. 2. The $|\Delta M| = 2$ region for all three derivatives (Fig 2, *left*) shows absorptive, nearly isotropic signals of line width 15 G (ΔH_{pp}) and g values of 4.038, 4.038, and 4.048 for Zn, Sn, and H cyt *c*, respectively.

The spectrum at 4 K in the $|\Delta M| = 1$ region for Zn cyt *c* (Fig. 2 *A*, *right*) exhibits a typical six-line pattern characteristic of a randomly oriented nondegenerate triplet state with rhombic symmetry and possessing well-defined ZFS parameters, $|D|$ and $|E|$, of 342×10^{-4} and 73×10^{-4} cm^{-1}, respectively. The spectral line shapes are narrow, showing that the geometry of the site is quite constrained and that there is effectively only one species. The polarization pattern from low field to high field is aaa–eee.

The Sn cyt *c* spectrum at the same temperature (Fig. 2 *B*, *right*) also shows spin polarization for the Z transitions, indicating that ISC occurs with some degree of spin selectivity; however, because of the less well-resolved and partially

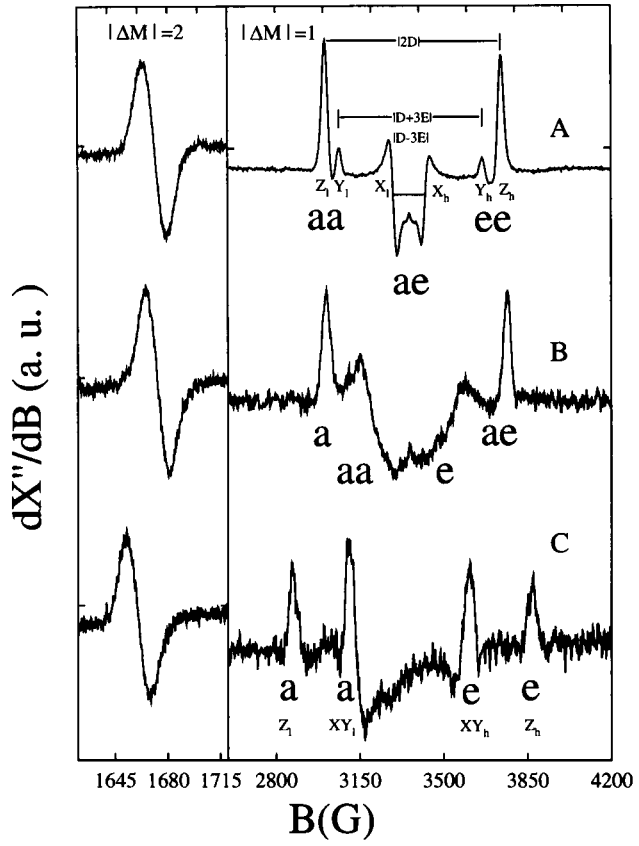

FIGURE 2 *X*-band EPR of the photoactivated triplet state of Zn, Sn, and free-base cyt *c* at 4 K. Experimental conditions for $|\Delta M = 1|$ region: (*A*) 500-mM Zn cyt *c* in 50% glycerol aqueous glass, 50-μM KCl pH 7, microwave power 2 uW, modulation amplitude 20 G (100 kHz); (*B*) 1-mM Sn cyt *c* in 50% glycerol aqueous glass, 50-mM KCl pH 7, microwave power 2 μW, modulation amplitude 20 G (100 kHz); (*C*) 1-mM free-base cyt *c* in 50% glycerol aqueous glass, 50-mM KCl pH 7, microwave power 2 μW, modulation amplitude 20 G (100 kHz); $|\Delta M = 2|$ region: (*A*) microwave power 50 μW, (*B*) microwave power 50 μW, (*C*) microwave power 100 μW. For A–C the modulation amplitude is 10 G (100 kHz). a indicates an absorptive transition and e an emissive transition.

thermalized high-field *XY* region of the Sn cyt *c* triplet spectrum at 4 K, the exact nature of ISC cannot be determined. A $|D|$ value of 353×10^{-4} cm^{-1} is obtained at this temperature. In contrast to those for the triplet in Zn cyt *c*, the canonical *X* and *Y* transitions of the spectrum are broadened even at 4 K, indicating environmental disorder at the porphyrin site or motional broadening of the vibronic triplet states. The $|E|$ value can be estimated to be $\sim 60 \times 10^{-4}$ cm^{-1}.

The spectrum at 4 K for H cyt *c* (Fig. 3 *C*, *right*) demonstrates a four-line "powder" pattern with a ZFS parameter $|E|$ of approximately zero. Such a case arises when there is in-plane symmetry. The polarization pattern of the free-base derivative from low field to high field is aa–ee. A $|D|$ value of 465×10^{-4} cm^{-1} is obtained for H cyt *c*.

For Zn cyt *c* the triplet EPR spectral features were independent of concentration in the range 30 μM to 1 mM. For reasons of sensitivity, only concentrations >100 μM could be used for the Sn and free-base derivatives, but their spectra too showed an independence of concentration. It can be concluded that the porphyrin, by virtue of being buried in the heme crevice of cyt *c*, creates a system whereby the chromophore can be considered to be in an infinitely dilute matrix without the complication of chromophore–chromophore energy transfer.

Temperature dependence

Fig. 3 shows the $|\Delta M| = 1$ region of the triplet state of Zn cyt *c*, under steady-state illumination, as a function of

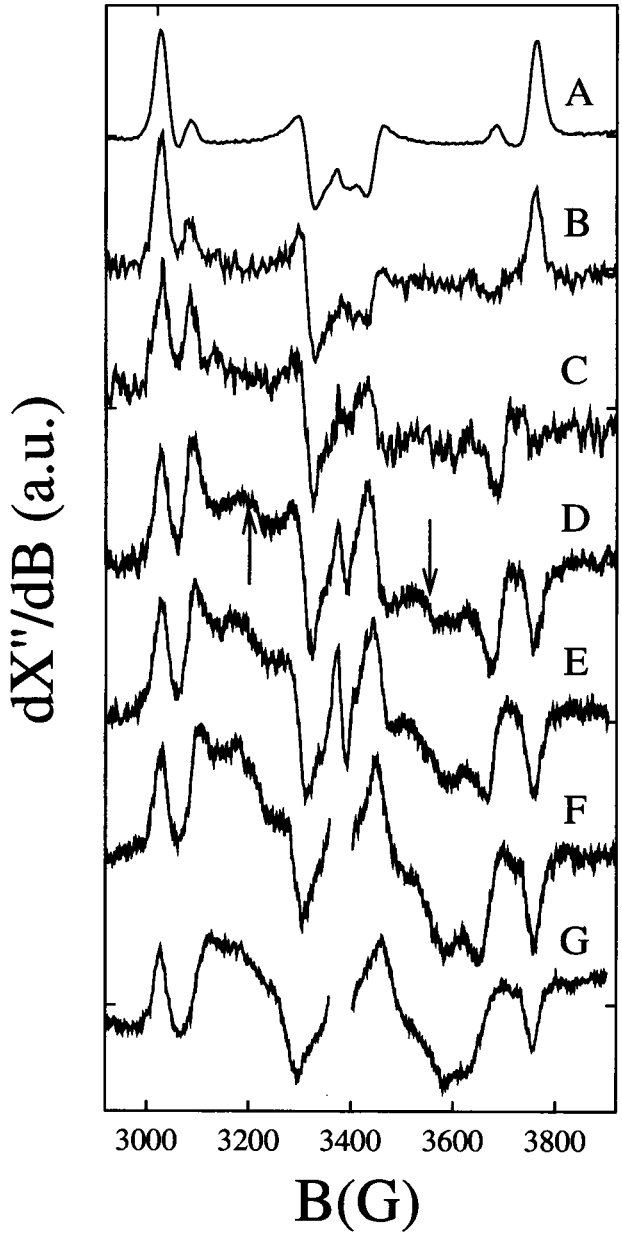

FIGURE 3 *X*-band EPR of the photoactivated triplet state of Zn cyt *c*. (*A*) 4 K, (*B*) 20 K, (*C*) 40 K, (*D*) 60 K, (*E*) 105K, (*F*) 130K, (*G*) 150 K. Experimental conditions: concentration ~1 mM in 50% glycerol aqueous glass, 50-mM KCl glass. Modulation amplitude 20 G, modulation frequency 100 kHz, and microwave power as follows: (*A*) 2 μW, (*B*) 10 μW, (*C*) 100 μW, (*D*) 10 mW, (*E*) 50 mW, (*F*) 100 mW, (*G*) 200 mW.

temperature. The ZFS parameter $|D|$ is independent of temperature from 4 to 150 K. The Z transition linewidth for the low-field and high-field transitions is 30 G and is also independent of temperature. A temperature dependence is seen in that the spin polarization, evident at 4 K, gives way to thermal equilibrium by 60 K, as indicated by the high-field emissions becoming absorptive in nature when the $|-1\rangle$ and $|+1\rangle$ spin sublevels become appreciably populated with increasing temperature (see Fig. 1). Consistent with this interpretation, the $|\Delta M| = 2$ transition signal demonstrates an increasing intensity relative to the $|\Delta M| = 1$ region with increasing temperature (data not shown). The line width for the Y and X transitions at 4 K are 26 and 34 G, respectively. Unlike the Z components of the field positions, which were invariant with temperature, the X and Y canonical transitions exhibit a temperature dependence, and the changes in line shape give evidence of motional broadening from 4 to 150 K. In this temperature range, the X and Y canonical transitions show a tendency to coalesce, and there is the emergence of transitions (shown by arrows in Fig. 3 D), indicating that there are triplet states possessing an effective axial symmetry, i.e., $|E| = 0$.

Fig. 4 (*inset*) shows the field positions of the canonical transitions X, Y, and Z determined from the data presented in Fig. 3. From these data, the ZFS parameters were determined. Fig. 4 shows a plot of the nonzero $|E|$ as a function of T^{-1}, with the solid curve representing the functional dependence of $|E|$ with temperature given by Eq. 5 with a JT splitting, δ_{JT}, of 180 cm^{-1}.

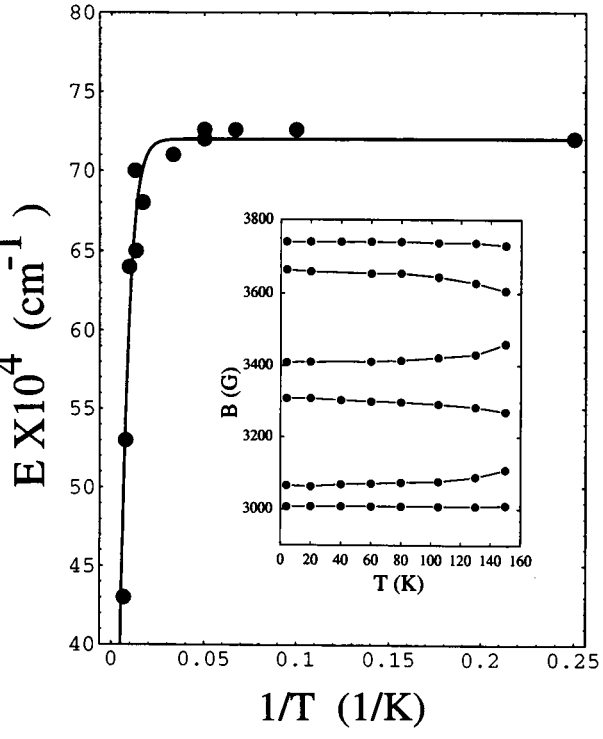

FIGURE 4 E zero-field splitting parameter as a function of reciprocal absolute temperature (K^{-1}) for Zn cyt c. ●, Experimental conditions given in Fig. 2. Solid curve, a fit to 73 tanh $(180/2k_BT)$. Inset: stationary field position as a function of temperature.

The $|\Delta M| = 1$ region of the photoactivated triplet state of Sn cyt c as a function of temperature is presented in Fig. 5. The $|D|$ ZFS parameter, as in Zn cyt c, is independent of temperature over the range 4–60 K. At 4 K the high-field Y transition is absorptive, signifying that at 4 K there is not the degree of non-Boltzmann entry into the triplet manifold that exists for the Zn derivative. By 60 K there is almost complete coalescence of the X and Y transitions, yielding an axially symmetric line shape ($E = 0$). An estimated value of $|E|$ of approximately 60×10^{-4} cm^{-1} was obtained from the 10- and 20-K spectra, where the X and Y transitions are visible (shown by the asterisks in Fig. 5). Because axial symmetry is achieved by 60 K, the JT splitting can be

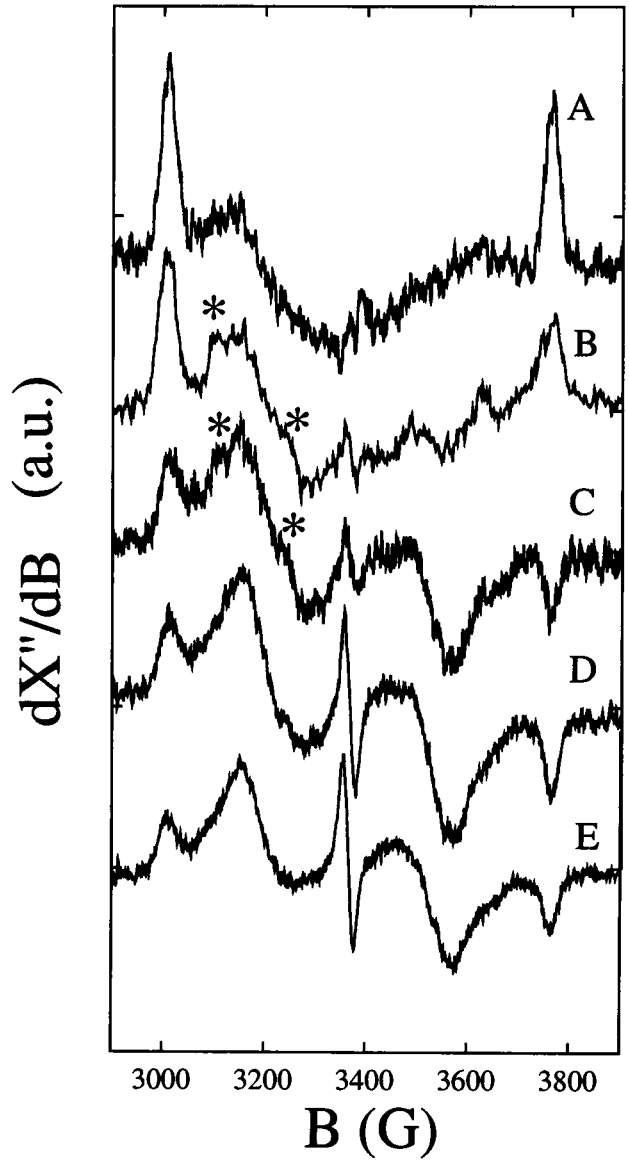

FIGURE 5 X-band EPR spectra of the photoactivated triplet state of Sn cyt c. (A) 4 K, (B) 10 K, (C) 20 K, (D) 40 K, (E) 60 K. Experimental conditions: concentration ~1 mM in 50% glycerol aqueous glass, 50-mM KCl, pH 7, modulation amplitude 20 G, modulation frequency 100 kHz, microwave power (A) 2 μW, (B) 10 μW, (C) 500 μW, (D) 5 mW, (E) 20 mW.

estimated to be $\geq 40\ cm^{-1}$. The line width for the Z transitions of Sn cyt c is 30 G.

The EPR spectra of the triplet state of H cyt c at various temperatures are shown in Fig. 6. The $|D|$ value was found to be $465 \times 10^{-4}\ cm^{-1}$. This value compares favorably with those of free-base porphyrins in model systems; for example the $|D|$ value for free-base mesoporphyrin in solvent at 77 K is $480 \times 10^{-4}\ cm^{-1}$ (van der Waals et al., 1979). The $|E|$ ZFS parameter over the entire temperature range is, within experimental error, zero. The sample exhibits spin polarization, which is essentially relieved by 20 K; but, interestingly, the XY high-field emissive transition attains thermal equilibrium before the Z high-field transition (compare Fig. 6 C and D). This would indicate an anisotropy in the spin lattice relaxation. The line widths for the Z and XY transitions are 37 and 69 G, respectively. No changes in the line widths were seen over this temperature range.

Comparison with metalloporphyrin model compounds

To examine what parameters of the spectra are affected by the protein, the photoactivated excited triplet of porphyrin model compounds under various conditions were compared with the porphyrin proteins. The $|\Delta M| = 1$ region of the photoactivated triplet state of ZnMP (mesoporphyrin IX dimethyl ester) is shown for the sample in two solvents (Fig. 7 A and B) and at two temperatures (Fig. 7 B and C). The $|D|$ values are the same regardless of solvent, but the spin polarization is different; in 100% toluene the spectrum

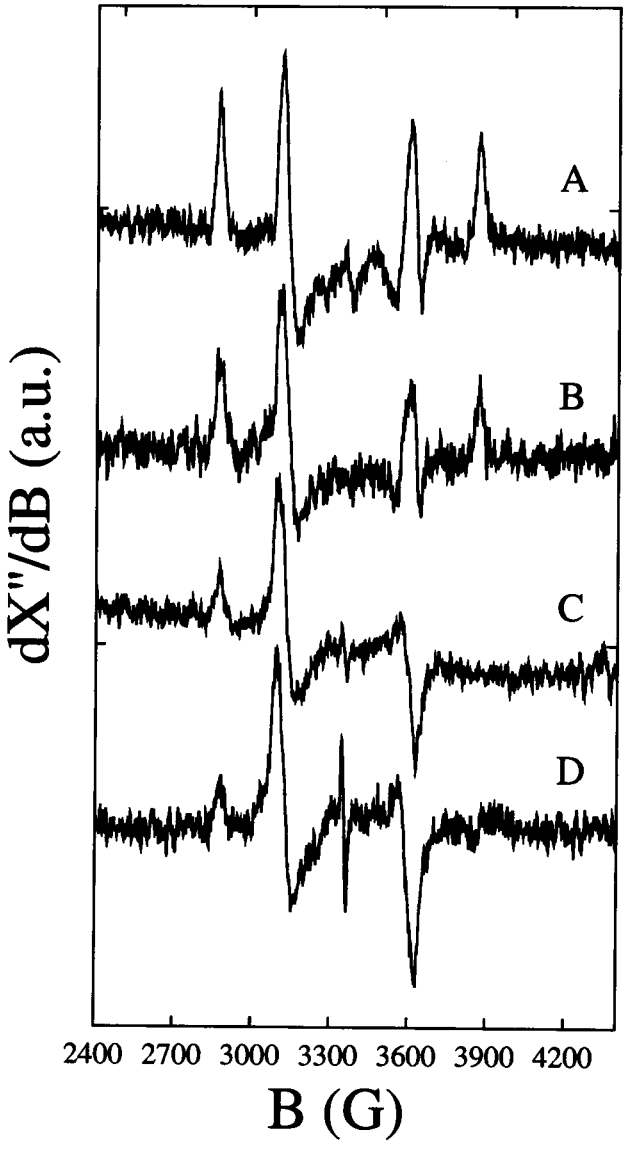

FIGURE 6 X-band EPR spectra of the photoactivated triplet state of porphyrin (free-base) cytochrome c. (A) 4 K, (B) 10 K, (C) 20 K, (D) 40 K. Experimental conditions: concentration ~1 mM in 50% glycerol aqueous glass, 50-mM KCl pH 7, modulation amplitude 20 G, modulation frequency 100 kHz, microwave power (A) 2 μW, (B) 5 μW, (C) 50 μW, (D) 1 mW.

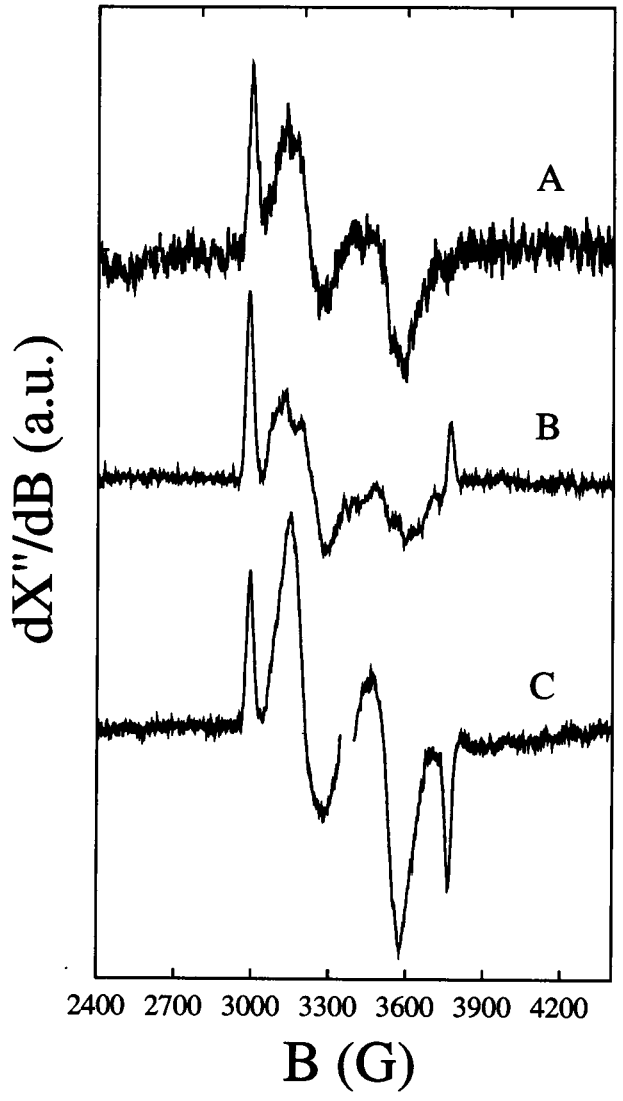

FIGURE 7 X-band EPR spectra of the photoactivated triplet state of ZnMP: (A) in 100% toluene glass at 4 K, microwave power 2 μW, (B) in 10% pyridine-toluene glass at 4 K, microwave power 2 μW, (C) in 10% pyridine-toluene glass at 77 K, microwave power 1 mW. ZnMP concentrations were approximately 500 μM.

showed decreased spin polarization at 4 K (Fig. 7 *A*), in contrast to the sample containing pyridine (Fig. 7 *B*). Coalescence of the *X* and *Y* canonical directions is evident in going from 4 to 77 K (Fig. 7 *B* and *C*). This coalescence occurs at a much lower temperature than for Zn cyt *c*, as can be seen by the contrast between its spectra at 60 and 105 K (Fig. 3) with that of MP (Fig. 7 *C*).

The excited triplet spectrum of Zn PP (protoporphyrin IX dimethyl ester) is shown at two temperatures in Fig. 8. The spectrum at 4 K shows spin polarization with a polarization pattern of aaa–eee, which is relieved by 77 K. At 77 K, in contrast to the spectrum for Zn MP (Fig. 7 *C*), the spectrum for ZnPP shows motional broadening in the *X* and *Y* canonical transitions, but coalescence is incomplete (Fig. 8 *B*), indicating that $\delta_{JT} > 50\ cm^{-1}$.

Finally, the EPR spectra of the triplet state of Sn MP and Sn PP in two solvents at 4 K are shown in Fig. 9. At this temperature the spin polarization is less significant than for

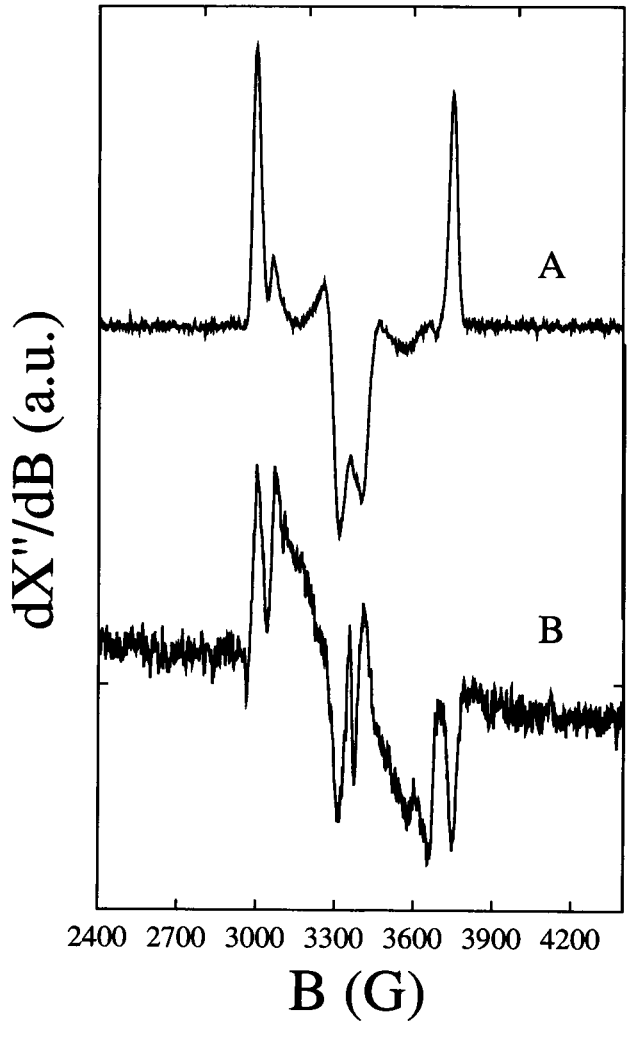

FIGURE 8 *X*-band EPR spectra of the photoactivated triplet state of ZnPP: (*A*) in 10% pyridine-toluene glass at 4 K, microwave power 2 μW, (*B*) in 10% pyridine-toluene glass at 77 K, microwave power 1 mW. Modulation amplitude in all spectra was 20 G (100 kHz). ZnPP concentrations were approximately 1 mM.

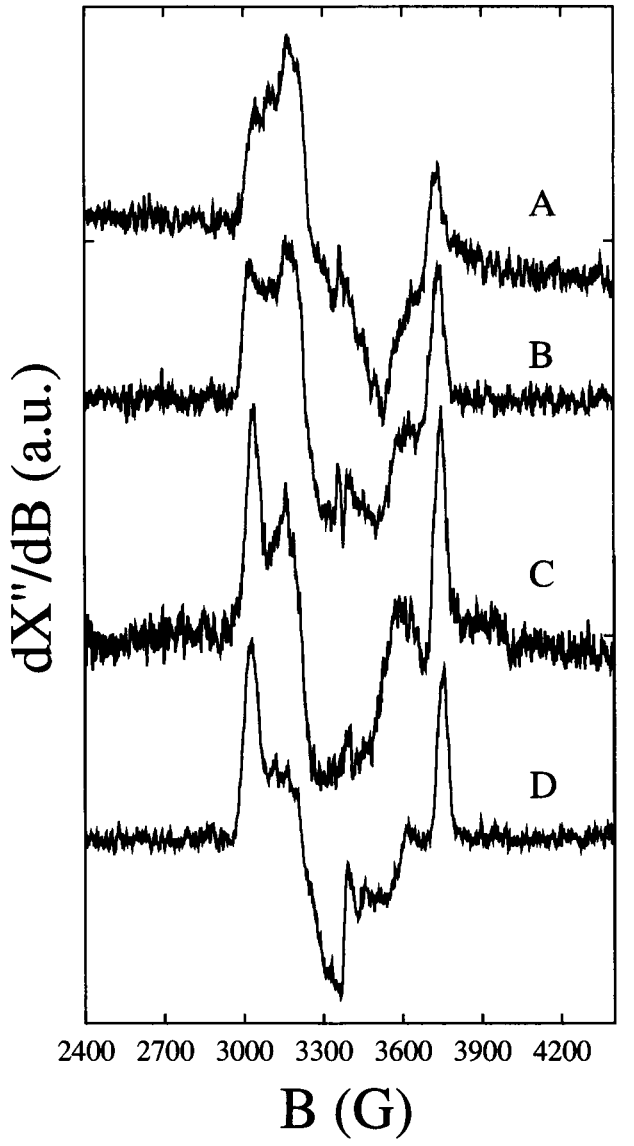

FIGURE 9 *X*-band EPR spectra of the photoactivated triplet state of Sn porphyrin model compounds: (*A*) SnMP in 50% pyridine-toluene glass at 4 K, microwave power 50 μW, (*B*) SnMP in dimethylformamide at 4 K, microwave power 20 mW, (*C*) SnPP in 50% pyridine-toluene glass at 4 K, microwave power 20 μW, (*D*) SnPP in dimethylformamide at 4 K, microwave power 20 μW. Modulation amplitude in all spectra was 20 G (100 kHz). All concentrations were approximately 4 mM.

the corresponding Zn derivatives. From the *X*, *Y* regions there is demonstrated dynamic behavior, indicating that for these Sn models the JT splitting is small and of the order of k_BT at 4 K. This is in stark contrast to the behavior of Zn derivatives in general, where the JT splittings (especially for ZnPP) are larger. The $|D|$ values for SnMP and SnPP are also larger than that found for Sn cyt *c* (Table 1).

To summarize, the values of the ZFS parameters that were found in our study are tabulated in Table 1. The ZFS parameters for Zn cyt *c* found in this study are identical to those obtained from ODMR (Zang and Maki, 1990). ODMR is contingent upon non-Boltzmann distribution in the triplet manifold and thus is limited to small excursions in temperature above 4 K. With EPR we were able to show that the $|D|$

TABLE 1 Zero-field splittings and phosphorescence lifetimes

	T (K)	|D|[a]	|E|[a]	Solvent	lifetime (ms)[b]	Reference[c]
Transition						
$a_{1g} \rightarrow e_g$		360	±166			1
$a_{2u} \rightarrow e_g$		203	−100–+66			1
$b_{2u} \rightarrow e_g$		417	±100			1
Compound						
Zn cyt *c*	4.2	342	73	glycerol/H_2O	20	2
Zn cyt *c*	150	342	43, 0[d]	glycerol/H_2O		2
Zn cyt *c*[e]	1.2	343	73	glycerol/H_2O		3
Zn PPHb	4.2	365	57	glycerol/H_2O		4
Zn MPHb	4.2	383	37	glycerol/H_2O		4
Zn PPMb	4.2	348	69	glycerol/H_2O		4
Zn MPMb	4.2	372	64	glycerol/H_2O		4
Zn PPHb	77	358, 364[d]	~47, 50[d]	glycerol/H_2O		4
Zn MPHb	77	360, 378[d]	0	glycerol/H_2O		4
Zn PPMb	77	349	70	glycerol/H_2O		4
Zn MP	4	361	b	50% pyr/tol	50	2
Zn MP	77	361	0	50% pyr/tol		2
Zn PP	4	351	70	50% pyr/tol	50	2
Zn PP	77	349	65, 0[d]	50% pyr/tol		2
Sn cyt *c*	4.2	355	b	glycerol/H_2O	17	2
Sn cyt *c*	10	352	56, 0[d]	glycerol/H_2O		2
Sn cyt *c*	77	354	~0	glycerol/H_2O		2
Sn MP	4	333	b	DMF	24	2
Sn MP	4	320	b	50% pyr/tol	24	2
Sn PP	4	336	b	DMF	18	2
Sn PP	4	332	b	50% pyr/tol	19	2
H cyt *c*	4.2–30	465	0	glycerol/H_2O	7	2
H_2P[e]	1.3–4.2	435, 440[d]	63, 69[d]	*n*-octane		5
H_2P	77	437	64	ethanol		5
H_2TPP	100	369	82	ethanol/ether		6
H_2MP	77	480	<5	ethanol		5

[a] $\times 10^{+4} \pm 0.001$ cm^{-1}.

[b] Lifetimes at 77 K, ±0.002 s.

[c] References: 1, Langhoff et al., 1975; 2, this work; 3, Zang, L., and A. H. Maki, 1990; 4, Hoffman, 1975; 5, cited by van der Waals et al., 1979; 6, Levanon and Wolberg, 1974.

[d] Multiple sites or apparent *E* values.

[e] ZFS obtained by ODMR.

Abbreviations used: Hb, hemoglobin; Mb, myoglobin; pyr, pyridine; tol, toluene; DMF, dimethyl formide; b, broad.

value for Zn cyt *c* is independent of temperature in the range 4–150 K. Literature data on porphyrin derivatives of other heme proteins and pertinent model compounds are also given in Table 1.

Phosphorescence lifetimes were measured for the cyt *c* derivatives, and relevant model compounds and the values are likewise given in Table 1.

DISCUSSION

Porphyrin triplet state in cytochrome *c*

The excited triplet paramagnetic state has been demonstrated in numerous systems to be a informative tool for the study of the structure and the dynamics of matrix interactions (Vanderkooi and Berger, 1989). The literature is replete with studies of porphyrin triplet states using magnetic resonance techniques (Levanon and Norris, 1978; Budil and Thurnauer, 1991); however, to date, the only EPR study performed on the excited triplet states of cyt *c* derivatives has been that of Zang and Maki (1990), who used ODMR. In a related study, Hoffman (1975) studied the photoactivated triplet state by EPR of the zinc porphyrin derivatives of myoglobin and hemoglobin.

For all three porphyrin derivatives of cyt *c*, the temperature independence of the $|D|$ ZFS parameter and the width of the *Z* transition lines demonstrate that there are no large protein conformational changes on the time scale of the EPR measurement in the vicinity of the chromophore over the temperature ranges studied, which in the case of Zn cyt *c* ranged from 4 to 150 K. The *XY* regions of the line shape, as a consequence of the vibronic nature of the ^3E triplet state, serves as a more sensitive indicator of local chromophore–matrix interactions (see below). With respect to line width, for both Zn and H cyt *c* the transitions at 4 K are relatively narrow and indicate primarily a single species of triplet. For Sn cyt *c* at 4 K, the line width of the *Z* transitions and the apparent line widths of the *X* and *Y* transitions are larger than for the Zn derivative, indicating a greater degree of inhomogeneous broadening; however, the *XY* regions might be obscured by the dynamic JT mechanism already in progress at 4 K. Local chromophore dynamics, as indicated by the

line-shape changes occurring in the *XY* regions over the same temperature excursion, do occur and will be discussed below. The results do not discount, however, motions or interactions of the chromophore protein or of the excitation per se that might occur on time scales much slower than that interrogated by EPR and as a consequence would contribute to the inhomogeneous broadening.

The narrowness of the transitions gives some indication about the order of the protein environment. It has been established by two-dimensional nuclear magnetic resonance that the ligation and structure of Zn cyt *c* are nearly identical to those of the native Fe(II) cyt *c*, and therefore one can suspect that there is not a great deal of disorder around the porphyrin (Anni et al., 1995). For the Sn cyt *c* derivative the two extra positive charges of the Sn(IV) may destabilize the protein, leading to a greater degree of inhomogeneity. In addition the ligation of Sn cyt *c* is uncertain; because chloride ligates so strongly to Sn, there may even be one or two chloride ions ligated to the metal within the protein.

Influence of the protein on the ZFS

Langhoff et al. (1975) have correlated the *D* value with the nature of the electronic transition responsible for the lowest triplet state. The correlation between these two is given in Table 1. In light of the Langhoff calculations, the *D* values obtained for Zn cyt *c* and Sn cyt *c* are consistent with a triplet transition of $a_{1g} \rightarrow e_g$. A further point about the *D* value is that a comparison of the values of the ZFS parameters for Zn and Sn cyt *c* at 4 K indicates that the central metal has little or no effect on the triplet-state ZFS parameters. Although Sn does exhibit an effect on the luminescent properties of the porphyrin, as can be seen from this study and from other work (Leenstra, 1979), there is no significant effect on the ZFS parameters with Sn relative to lighter central metals, and thus the interaction that is due to spin orbit coupling contributes little, if any, to the ZFS of the lowest excited triplet in Zn and Sn porphyrin derivatives of cyt *c* (Table 1). Spin orbit coupling, however, is primarily responsible for intersystem crossing and therefore controls entry and exit of the triplet manifold.

In model systems, the value for $|D|$ depends upon the substituent groups. The $|D|$ value is 360×10^{-4} cm^{-1} for Zn porphine (ZnP) in *n*-octane, whereas 5,10,15,20-tetraphenylporphyrin(zinc) (Zn TPP) gives a value of 306×10^{-4} cm^{-1} (Table 1). Inasmuch as $|D|$ is inversely proportional to the average cubed distance between the two spins, $\langle r^3 \rangle^{-1}$ (Kleibeucker et al. 1978), the lower value for Zn TPP has been attributed to partial spin density on the lateral phenyl groups. (But we also note that time-resolved resonance Raman studies of Zn TPP have put to question the extent, if any, that delocalization extends onto the phenyl groups of metallo-TPP compounds (Walters et al., 1989; dePaula et al., 1992)). In the case of cytochrome *c*, the heme pocket is lined with aromatic residues. For instance, Trp-59, Phe-36, and Phe-82 are all within 5 Å of the heme (Bushnell et al., 1990). Therefore, it might be possible for the spin to be delocalized onto these residues. However, the experimentally determined $|D|$ value for Zn cyt *c*, which is larger than for the model compounds that have aromatic substituents, would indicate that the triplet excitation is confined primarily to the porphyrin ring and does not have an appreciable spin density on surrounding amino acid residues during the time scale of EPR.

There are smaller variations in the $|D|$ value between the model compounds and the proteins. The $|D|$ value for Zn cyt *c* is somewhat larger than for Zn porphine or Zn MP and is closer to Zn PP, a derivative in which there are two vinyl groups that are known to couple to the π system of the porphyrin ring (Table 1). On this basis it can be suggested that the porphyrin in Zn cyt *c* maintains partial spin delocalization comparable with those of the vinyl groups at the 2 and 4 positions of Zn PP.

Temperature dependence of EPR line shape and the dynamic Jahn–Teller effect

As a consequence of the fourfold symmetry of the metalloporphyrins, the lowest triplet state has ^3E_u symmetry. It follows, then, that the JT theorem should be operative, i.e., "orbital degeneracy and stability of nuclear configuration are incompatible unless all atoms of the molecule lie in a straight line" (Jahn and Teller, 1937). To achieve the JT splitting, however, the group must be perturbed by a substituent or asymmetric environment. For porphyrins, the JT active symmetries, b_{1g} and b_{2g}, can be thought of as in-plane distortions creating rectangular (along the pyrrole *N-N* axis) or diamond-shaped (along methine bridge axis) symmetry, respectively. Thus, the ZFS parameter, $|E|$, which would be conjectured to be zero for a square planar symmetry, will now take on nonzero values indicative of in-plane symmetry breaking driven by the JT instability.

All Zn and Sn porphyrin protein systems and model compounds studied possess nonzero $|E|$ values at cryogenic temperatures (Table 1). Because the occupation of the now nondegenerate triplet states should be temperature dependent according to the Boltzmann law, the JT splitting, δ_{JT}, may be assessed through the temperature dependence of the line shape in the region of the *X* and *Y* canonical transitions. This theory, although studied experimentally for mesitylene in *B*-trimethylborazole (deGroot et al., 1969) and zinc porphin in *n*-alkane host crystals (van Noort et al., 1982), has remained largely untested in porphyrin systems, especially in noncrystalline or amorphous systems. The $|E|$ ZFS parameter, given by the theory outlined in the introductory section and the discussion above, proves a sensitive indicator of environmental symmetry-breaking perturbations.

In this study, the dynamics of the canonical field positions, *X* and *Y*, of Zn cyt *c* were monitored as a function of temperature in the range 4–150 K (Fig. 3) and, using the derived nonzero *E* values, the maximum JT splitting can be estimated to be 180 cm^{-1} (Fig. 4). A question is: Is this value a reflection of interaction with the protein? To answer this, we compare with model porphyrins. In the biosynthesis of cyt *c*, the start-

ing protoporphyrin IX structure loses the vinyl groups by condensation with the Cys-14 and Cys-17 residues on the protein. As there is significant vinyl group coupling with the porphyrin core (Adar and Erecinska, 1974), MP, which lacks the vinyl groups, would be expected to be a better model for the study of cyt *c* than is PP. The ZnMP derivative demonstrates a line shape that even at 4 K possesses a component with an $|E|$ ZFS parameter that is essentially zero (Fig. 7); this translates to a JT splitting for Zn MP of ≥ 3 cm^{-1}, which is considerably lower than for Zn porphyrin in cyt *c*. It can therefore be concluded that the protein matrix of cyt *c* has stabilized one deformation of the porphyrin relative to the other. Similar drastic stabilization effects were noticed in ZnMP myoglobin (Hoffman, 1975). Zn PP in 50% pyridine-toluene, in contrast, shows no significant dynamic interconversion of the vibronic states until temperatures near 77 K (Fig. 8), indicating that the JT splitting is ≥ 50 cm^{-1}. In this case, it is hypothesized that the substituent vinyl groups perturb the symmetry, leading to a split in the triplet vibronic states.

Consequently, even though the vinyl groups of the porphyrin in cyt *c* are lost through condensation with the protein, there is an effect exerted by the protein cysteine residues or other factors particular to the heme crevice that serves to stabilize the lower vibronic state of the ^3E triplet state. The origin of the stabilization by the protein is most likely from the heme pocket environment rather than from ligation because it has been shown that there is an insensitivity of $|D|$ and $|E|$ values with different nitrogenous ligands (Hoffman, 1975). This was also observed for the EPR of the triplet state of Zn MP in a noncoordinating solvent (neat toluene) and in a system providing axial ligation (50% pyridine-toluene) (Fig. 7). The effects of ligand and matrix thus appear to more subtle than a simple gross changes in the ZFS parameters previously emphasized by this laboratory and others and may be reflected in JT splittings or relaxation rates.

The observation of the emergence of an $|E| = 0$ component along with broadening before the observation of the coalescence of the low-temperature *X* and *Y* canonical transitions deserves some comment. In a glassy matrix there will not be a sharp δ_{JT} splitting between the vibronic components of the triplet state but rather a distribution of splittings determined by the structure of the specific complex. The *D* and *E* values, however, are expected to be nearly the same for all molecules. This is borne out in the temperature profile of the Zn cyt *c* triplet. At low temperature, when $k_BT < \delta_{JT}$ (Fig. 3 *A*), all the molecules are in the lower vibronic state, with ZFS parameters as given in Table 1. Upon increasing the temperature to 60 K (~ 40 cm^{-1}) we see that the EPR spectrum shows that there is already a small fraction of the molecules that are undergoing dynamic processes. Given what is known regarding the population distribution of ground-state molecules of Zn cyt *c*, from fluorescence line narrowing studies (Logovinsky et al., 1993), it is anticipated that the distribution of δ_{JT} splittings will have a width (2σ of a Gaussian distribution) of at least 65 cm^{-1}, assuming perfect correlation between the first excited singlet state and the lowest excited triplet state.

The analysis of the temperature dependence of the EPR line shape of Sn cyt *c* and its corresponding model complexes is not so straightforward. The reason for this is that the *XY* region, where dynamic events would be reflected, is much broader than in Zn porphyrin species. Also it appears that the JT splittings, δ_{JT}, for Sn porphyrins are smaller than in Zn porphyrins. Both of these phenomena serve to complicate those regions of the spectra that yield the most information regarding spin dynamics. It is clear that the $|D|$ value for Sn cyt *c* is larger than in both Sn model compounds studied at 4 K. This suggests that in Sn cyt *c*, unlike in Zn cyt *c*, the spatial extent of the triplet excitation is more confined in the protein matrix than in the solvent systems studied.

From Fig. 9 it is evident that the Sn MP EPR spectrum at 4 K shows that the *XY* region is quite thermalized, and, judging by the large signal at field values corresponding to $|E| \approx 0$, both vibronic states of the triplet are appreciably populated. The latter observation allows an estimate of δ_{JT} to be of the order of k_BT at 4 K (≥ 3 cm^{-1}). Sn PP in two solvent systems (Fig. 9) also shows an appreciable signal at field values indicative of an axially symmetric species, $|E| \approx 0$, however, the PP complex with Sn exhibits a greater degree of spin polarization at 4 K. Sn cyt *c* has the same general line shape at 4 K as Sn PP insofar as spin polarization is concerned. The phosphorescence lifetimes at 77 K of Sn cyt *c* and the two models are experimentally the same, and therefore the increased degree of polarization in the Sn cyt *c* relative to the Sn model complexes can be attributed to spin–phonon interactions.

Electron spin polarization and spin lattice relaxation

Spin state dynamics can be obtained from the EPR excited triplet spectrum under steady-state illumination conditions. ISC in porphyrins proceeds through coupling of the electronic spin with the residual orbital angular momentum. As the orbital angular momentum is in reference to the molecular axis system, ISC is highly selective with respect to the zero-field spin states. Consequently, each spin state will have separate population, depopulation, and spin lattice relaxation rates (McGlynn et al., 1969).

Under steady-state illumination, the signal intensity for $|0\rangle \leftrightarrow |\pm 1\rangle$ transitions in the absence of any spin lattice relaxation (for a field direction parallel to one of the zero-field principal axes) is a function of the entry and decay rates into the triplet manifold and is described by

$$I_{\hat{u}}(\pm 1) = \pm\{p_{\hat{u}}(0)/k_{\hat{u}}(0)\} - \{p_{\hat{u}}(\pm 1)/k_{\hat{u}}(\pm 1)\}, \quad (5)$$

where $\hat{u}$ is a unit vector of the molecular axis frame directed along the field direction and $p_{\hat{u}}$ and $k_{\hat{u}}$ are the entry and exit rates for the spin level when the field is directed along the $\hat{u}$ direction (Ponte Goncalves and Spendel, 1977). If the $|0\rangle$ sublevel is more populated than the $|\pm 1\rangle$ sublevels, then

$I_{\hat{u}}(+1) > 0$ and $I_{\hat{u}}(-1) < 0$, where an $I(\pm 1) > 0$ represents an absorption and $I(\pm 1) < 0$ an emission of microwave power. Likewise, if the $|\pm 1\rangle$ sublevels are more populated than the $|0\rangle$ sublevel, the reverse condition will be operative. Without spin lattice relaxation, $|I_{\hat{u}}(+1)| = |I_{\hat{u}}(-1)|$. From the spin polarization pattern at low temperature where spin lattice relaxation can be considered negligible, the most active sublevel may be ascertained (Thurnaurer et al., 1975). In general, if the triplet lifetime for a particular sublevel is shorter than the spin lattice relaxation time connecting that sublevel with another sublevel, there will be a non-Boltzmann distribution among the triplet manifold of levels, and one or more of the transitions may exhibit an emissive signal. This non-Boltzmann distribution of the triplet state is called electron spin polarization (Hausser and Wolf, 1976). It is still possible to get electron spin polarization, i.e., $I_{\hat{u}}(+) \approx I_{\hat{u}}(-)$ with an appreciable rate of spin lattice relaxation, provided that

$$|p_{\hat{u}}(0)k_{\hat{u}}(\pm 1) - p_{\hat{u}}(\pm 1)k_{\hat{u}}(0)| \gg (T_1)^{-1}\left(\frac{\Delta}{k_B T}\right)(p_{\hat{u}}(0) + 2p_{\hat{u}}(\pm 1)), \quad (6)$$

where T_1 is the spin lattice relaxation time, Δ the energy splitting between $|0\rangle$ and $|\pm 1\rangle$, respectively, T is the absolute temperature, and k_B the Boltzmann constant.

Zn cyt *c* exhibits behavior typical of other Zn porphyrins in the mechanism governing ISC. The polarization pattern exhibited in Fig. 2 *A*, aaa–eee, is consistent with the spin selectivity of ISC predominantly into the $|T_z\rangle$ zero-field spin state. The triplet state EPR spectrum of Sn cyt *c* at 4 K (Fig. 2 *B*) has a polarization pattern that indicates non-Boltzmann entry when the magnetic field is parallel to the *Z* and *X*-axes (*Z* and *X* canonical transitions) but is partially thermalized in the *Y* transitions. We can conclude that in Sn cyt *c* the $|T_z\rangle$ is active; however, from the lack of resolution and partial thermalization of the high-field *XY* region we cannot say for sure what involvement the $|T_x\rangle$ and $|T_y\rangle$ spin sublevels will have. We can also conclude that H cyt *c*, with a polarization pattern of aa–ee at 4 K, also has both in-plane and out-of-plane active sublevels.

The transition from a non-Boltzmann distribution of spins within the triplet sublevels to thermal equilibrium is a function of the entry, exit, and spin relaxation rates. The transition to thermal equilibrium, in general, occurs at lower temperature for the Sn cyt *c* than for Zn cyt *c*. For Sn cyt *c* the high-field *Y* transition at 4 K already approaches thermalization, the high-field *X* emissive signal becomes absorptive by 10 K, and the high-field *Z* transition becomes absorptive by 20 K (Fig. 5). For Zn cyt *c*, however, spin polarization effects are maintained for the high-field *Z* transition up to temperatures exceeding 40 K, with the *X* and *Y* transitions undergoing thermalization by temperatures of approximately 20 and 40 K, respectively. Thus, for Zn cyt *c*, thermal equilibrium of the spin system with the protein is not established until approximately 60 K. Similar effects are seen in H cyt *c*, where the high-field emissive *XY* resonance thermalizes before the high-field emissive *Z* transition. Moreover, in both metalloderivatives an apparent anisotropy in spin lattice relaxation is evident from the observation that the three canonical transitions undergo thermalization transitions at different temperatures.

Equation 7 establishes the conditions under which spin polarization effects might be manifested, even with substantial spin relaxation with steady-state illumination. The phosphorescence lifetimes at 77 K for Sn cyt *c* and Zn cyt *c*, of 17 and 20 ms, respectively, are not sufficiently different to explain the line shape changes with temperature, assuming no temperature dependence in phosphorescence lifetime (Turro, 1991). Moreover, it has been determined that for Zn cyt *c* the decay constant is temperature independent in the range 15–200 K (Zang and Maki, 1990). Because the radiative lifetimes for both Zn cyt *c* and Sn cyt *c* are not significantly different and because the efficiency of triplet formation and phosphorescence quantum yield for both is also essentially the same at 77 K (Dixit et al., 1984), the observed differences seen in the triplet EPR spectrum of the Sn and Zn derivatives of cytochrome *c* are due to differences in the temperature dependence of the spin lattice relaxation times for each derivative, and hence for each derivative there exist different degrees of spin lattice, i.e., phonon, coupling.

Spin–phonon interactions, in general, have recently been an area of study to ascertain information on the phonon density of states of proteins (Allen et al., 1982; Wagner et al., 1985). The temperature dependence of the spin lattice relaxation can be related to the phonon density of states, and hence structural and dynamic properties may be obtained. Insofar as heme, blue copper, and iron-sulfur proteins are concerned, an anomalous temperature dependence (T^n, $5.22 < n < 6.22$) of the spin lattice relaxation has been observed for paramagnetic centers with an odd number of electrons (Kramers states) (Herrick and Stapleton, 1976; Drews et al., 1990; Bertrand and Gayda, 1982). The nonintegral nature of the power-law exponents describing the temperature dependence of the spin lattice relaxation time has been interpreted in terms of "lattice" structures of a non-Euclidean (fractional) dimension, or more currently to a modification of the Debye density of states (Elber and Karplus, 1986; Krumhansl, 1986; Stevens and Stapleton, 1990). The temperature dependence of the high-resolution optical transitions has similarly been interpreted in terms of coupling between porphyrins and proteins. In case of porphyrin-substituted horseradish peroxidase, hole burning and spectral diffusion during temperature cycling showed steplike behavior, which suggested that there were a small number of discrete two-level systems with which the chromophore interacts (Zollfrank et al., 1991). The spectral diffusion of Zn cyt *c* was studied by photon echo experiments in which the optical dephasing time was directly obtained and nonexponential behavior was interpreted in terms of small fluctuations between substates (Leeson et al., 1994). The temperature dependence of resolution in fluorescence line-narrowed spectra of Zn cyt *c* has also been measured, and resolution is abolished at ~40°C (Logovinsky et al., 1993). It is clear

from this body of work involving EPR and optical measurements that the relaxation of excited species in proteins must be coupled to particular modes within the protein and that the number and energies of these modes must be finite.

In this study, a triplet state ($S = 1$, non-Kramers state) was investigated in a protein environment, and although it is apparent from the temperature dependence of the abolishment of spin polarization that there are marked differences between the relaxation rates among the triplet sublevels in an applied magnetic field, quantification of rates and temperature dependencies awaits direct measurement of the spin lattice relaxation times. Preliminary progressive power saturation studies of Zn cyt *c* have revealed a weak dependence of $P_{1/2}$ on temperature and that between 4 and 40 K (Angiolillo, unpublished observation). $P_{1/2}$ is related to $(H_{1/2})^2$, which is related to $[(g_e\beta_e)^2T_1T_2]^{-1}$, where T_1 and T_2 are the spin lattice and spin–spin relaxation times, respectively, and g_e and β_e are as previously described. The literature is inconclusive regarding the behavior of $S = 1$ spin lattice relaxation, and it appears the relaxation behavior is quite different in crystalline and disordered matrices (Gradl and Friedrich, 1987; Sims et al., 1972; Schwoerer et al., 1972). These data suggest that the triplet-state spin lattice relaxation rates do not follow current theories used to describe the temperature dependence of spin–phonon interactions in transition metals (Abragam and Bleaney, 1970).

Free-base cyt *c* (H cyt *c*)

In free-base porphyrins the fourfold axis of symmetry responsible for the degeneracy of the triplet state in metalloporphyrins and the dynamic JT effect is relieved. Consequently, the lowest excited triplet state is nondegenerate. Inasmuch as the JT effect is inoperable, the line shape would be predicted to be temperature independent (excluding spin polarization effects) and have a nonzero $|E|$ ZFS parameter. The triplet EPR spectrum of the $|\Delta M| = 1$ region as a function of temperature for H cyt *c* is shown in Fig. 6. Surprisingly, the spectrum demonstrates cylindrical symmetry, with $|D|$ and $|E|$ values of 465×10^{-4} cm^{-1} and ≈ 0, respectively. Moreover, the ZFS parameters remain constant over the temperature range studied.

Although cylindrical symmetry of the zero-field tensor has been noticed in free-base porphyrin model compounds such as octaethylporphyrin in dichloromethane/ethanol ($T = 120$ K) (Levanon et al., 1993) and hematoporphyrin IX in 5% pyridine/ethanol (Lhoste et al., 1967), for the most part free-base porphyrins show definite rhombic symmetry ($E \neq 0$) in the ZFS parameters. Tetraphenylporphyrin in ether/ethanol ($T = 100$ K), for instance, has ZFS parameters of $|D| = 369 \times 10^{-4}$ cm^{-1} and $|E| = 82 \times 10^{-4}$ cm^{-1}, respectively, indicating a rather large departure from axial symmetry (Levanon and Wolberg, 1974).

The explanations for the persistence of cylindrical symmetry of the zero-field tensor in some of the free-base porphyrins have ranged from proton movement (tautomerization) resulting in an averaging out of the in-plane anisotropy to the possibility that the perturbation induced by replacement of the central metal by two pyrrole hydrogens is insufficient to relieve the cylindrical symmetry of the ZFS tensor, much like the ineffectiveness of lateral substituents (Lhoste et al., 1967). The latter explanation is unlikely because the two protons have a drastic effect on the Q-band optical transitions.

With respect to proton migration, most previous studies of free-base porphyrins have been performed at relatively higher temperatures where thermal activation might be envisaged. Ground-state proton movement in porphyrins has been demonstrated and extensively studied both theoretically and experimentally (Sarai, 1982; Bersuker and Polinger, 1984; Braun et al., 1994) and is not a possibility at temperatures in the range studied. If the protons are moving at this temperature fast enough to average the in-plane anisotropy on the EPR time scale, then a maximum $|E|$ value of $1/3\ |D|$, where $|D|$ is of the order of 460×10^{-4} cm^{-1}, would require that the "hopping" rate be of the order of 10^9 s^{-1} or faster ($\nu \gg g_e\beta_e 3E/h$). Low-temperature (4.2-K) high-resolution fluorescence of free-base porphin incorporated into an *n*-octane Shpol'skii matrix clearly reveals that excited-state phototautomerization of the pyrrole hydrogens occurs and that it appears to be a nonthermally activated process (Volker and van der Waals, 1976). Free-base porphyrin in another protein, horseradish peroxidase, is known to undergo a photoinduced proton transfer reaction at liquid-helium temperature, as indicated by high-resolution fluorescence spectroscopy (Fidy et al., 1989) and absorption (Fidy et al., 1992) measurements. This reaction has not been studied in H cyt *c*, but such a reaction would likely be a general occurrence in porphyrins. Whether the phototautomerization occurs in the excited singlet or the triplet state, or both, is not known, but the observation that the *XY* equivalence of the porphyrin in the triplet state suggests that a photoreaction in the triplet state could account for the observed phototautomerization. Phosphorescence-detected magnetic resonance of free-base protoporphyrin IX in a polycrystalline *n*-octane matrix at 5 K (Suisalu and Avarma, 1983) and EPR of free-base porphin in single crystal *n*-octane (van der Waals et al., 1979) both reveal nonzero $|E|$ ZFS values and thus indicate that if phototautomerization is occurring it is on a time scale slower than that given by the splitting of the *X* and *Y* canonical transitions. This is not an unlikely possibility in the nonpolar environment of *n*-octane. Further studies of these systems including the effects of deuteration and fluorescence anisotropy decay measurements are currently under way.

CONCLUSIONS

Several conclusions can be drawn from this study: (i) In the case of all three derivatives of cyt *c* spin–orbit intersystem crossing can account for the observed polarization patterns in the triplet EPR spectra at low temperature. From the spin polarization pattern per se, it can also be concluded that the $|T_z\rangle$ spin sublevel is active with respect to selective ISC for

all three derivatives of cyt *c* and that for Zn cyt *c* it is the predominant sublevel of entry. (ii) The temperature independence of the $|D|$ ZFS parameter for Zn, Sn, and H cyt *c* suggests that no delocalization of the triplet excitation occurs on the time scale of EPR and that no large conformational changes are indicated over the temperature range studied. (iii) The large low-temperature $|E|$ ZFS parameter for Zn cyt *c*, the largest thus reported for Zn-substituted heme proteins, indicates that the protein environment imposes an asymmetric field at the porphyrin. Also, for Zn cyt *c*, based on ZFS parameters and spin polarization characteristics, Zn PP appears to be a better model compound than Zn MP. (iv) The temperature-dependent line-shape changes observed in the *XY* regions of Zn and Sn cyt *c* can be accounted for by the vibronic coupling theory of a JT unstable degenerate triplet state. For Zn cyt *c* we have determined a maximum JT splitting of the vibronic triplet states to be approximately 180 cm^{-1}, indicating that the protein matrix stabilizes the lower vibronic state. (v) The triplet state for H cyt *c* surprisingly yielded a cylindrically symmetrical EPR spectrum ($|E| \approx 0$) at all temperatures studied (4–40 K). A possible explanation for this observation is the excited-state migration of the pyrrole hydrogens. (vi) There are indications from the temperature dependence of the electron spin polarization and microwave progressive power saturation data that the triplet states in these proteins exhibit relaxation phenomena not easily explained by the standard theories used to describe transition-metal paramagnetic relaxation.

The work was supported by NIH grants GM 34448 and PO1 GM48130. The Johnson Research Foundation supplied the EPR equipment. This work, done by P. J. A., was in partial fulfillment of the requirements of the Ph.D. degree. The authors wish to express their thanks to W. Wright for help in the preparation of the protein derivatives.

REFERENCES

Abragam, A. and B. Bleaney. 1970. Electron Paramagnetic Resonance of Transition Ions. Dover Press. New York. 541–574.

Adar, F., and M. Erecinska. 1974. Resonance Raman spectra of the *b*- and *c*-type cytochromes of succinate-cytochrome *c* reductase. *Arch. Biochem. Biophys.* 165:570–580.

Allen, J. P., J. T. Colvin, D. G. Stinson, C. P. Flynn, and H. J. Stapleton. 1982. Protein conformation from electron spin resonance relaxation data. *Biophys. J.* 38:299–310.

Angiolillo, P. J., J. S. Leigh, and J. M. Vanderkooi. 1982. Resolved emission spectra of iron-free cytochrome *c*. *Photochem. Photobiol.* 36:133–137.

Anni, H., J. M. Vanderkooi, and L. Mayne. 1995. Structure of Zn-substituted cytochrome *c*: nuclear magnetic resonance and optical spectroscopic studies. *Biochemistry.* 34:5744–5753.

Bersuker, G. I., and V. Z. Polinger. 1984. The pseudo-Jahn-Teller dynamics of central protons in porphins. *Chem. Phys.* 86:57–65.

Bertrand, P., and J-P. Gayda. 1982. Electron spin-lattice relaxation of the (4Fe–4S) ferrodoxin from *B. Stearothermophilus*. Comparison with other iron proteins. *J. Chem. Phys.* 76:4715–4718.

Braun, J., M. Schlabach, B. Wehrle, M. Kocher, E. Vogel, and H. Limbach. 1994. NMR tautomerism of porphyrin including the kinetic HH/HD/DD isotope effects in the liquid and the solid state. *J. Am. Chem. Soc.* 116: 6593–6604.

Budil, D. E., and M. C. Thurnauer. 1991. The chlorophyll triplet state as a probe of structure and function in photosynthesis. *Biochim. Biophys. Acta.* 1057:1–41.

Bushnell, G. W., G. V. Louie, and G. D. Brayer. 1990. High-resolution three-dimensional structure of horse heart cytochrome *c*. *J. Mol. Biol.* 214:585–595.

Carrington, A., and A. D. McLachlan. 1967. Introduction to Magnetic Resonance. Chapman & Hall, London. Chapter 12.

Casimiro, D. R., L.-L. Wong, J. L. Colón, T. E. Zewert, J. H. Richards, I.-J. Chang, J. R. Winkler, and H. B. Gray. 1993. Electron transfer in ruthenium/zinc porphyrin derivatives of recombinant human myoglobin and cytochrome *c*. *J. Am. Chem. Soc.* 115:1485–1489.

de Groot, M. S., I. A. Hesselmann, and J. H. van der Waals. 1969. Paramagnetic resonance in phosphorescent aromatic hydrocarbons. VI. Mesitylene in *B*-trimethylborazole. *Mol. Phys.* 1:61–68.

de Paula, J. C., V. A. Walters, C. Nutaitus, J. Lind, and K. Hall. 1992. Transient resonance Raman spectrum of meso-tetraphenylporphine: an analysis of chemical factors that influence the dynamics of the excited states of metalloporphyrins. *J. Phys. Chem.* 96:19591–10594.

Dixit, B. P. S. N., V. T. Moy, and J. M. Vanderkooi. 1984. Reactions of excited state cytochrome *c* derivatives. Delayed fluorescence and phosphorescence of zinc, tin and metal-free cytochrome *c* at room temperature. *Biochemistry.* 23:2103–2107.

Drews, A. R., B. D. Thayer, H. J. Stapleton, G. C. Wagner, G. Giuglirelli, and S. Cannistraro. 1990. Electron spin relaxation measurements on the blue-copper protein plastocyanin. *Biophys. J.* 57:157–162.

Elber, R., and M. Karplus. 1986. Low-frequency modes in proteins: use of effective-medium approximation to interpret the fractal dimension observed in electron-spin relaxation experiments. *Phys. Rev. Lett.* 56:394–397.

Elias, H., M. H. Chou, and J. R. Winkler. 1988. Electron-transfer kinetics of Zn-substituted cytochrome *c* and its $Ru(NH_3)_5$(histidine-33) derivative. *J. Am. Chem. Soc.* 110:429–434.

Fidy, J., K.-G. Paul, and J. M. Vanderkooi. 1989. The mechanism of phototautomerization in mesoporphyrin horseradish peroxidase. Studies by fluorescence line-narrowing spectroscopy. *J. Phys. Chem.* 93:2253–2261.

Fidy, J., J. M. Vanderkooi, J. Zollfrank, and J. Friedrich. 1992. More than two pyrrole tautomers of mesoporphyrin stabilized by a protein. High resolution optical spectroscopic study. *Biophys. J.* 61:381–391.

Friedrich, J., J. Gafert, J. Zollfrank, J. M. Vanderkooi, and J. Fidy. 1994. Spectral hole burning and selection of conformational substates in chromophores. *Proc. Natl. Acad. Sci. USA.* 91:1029–1033.

Gradl, G., and J. Friedrich. 1987. Electron-spin-lattice relaxation of photoexcited triplet states in disordered solids. *Phys. Rev. B.* 35:4915–4921.

Hameka, H. F., and N. J. Oosterhoff. 1958. The probabilities of triplet-singlet transitions in aromatic hydrocarbons and ketones. *Mol. Phys.* 1:358–371.

Hausser, K. H., and H. C. Wolf. 1976. Optical spin polarization in molecular crystals. *Adv. Mag. Res.* 8:85–121.

Herrick, R. C., and H. J. Stapleton. 1976. Anomalous T^7 Raman spin-lattice relaxation rate of low spin cytochrome P-450 from *Pseudomonas putida*. *J. Chem. Phys.* 65:4778–4785.

Hoffman, B. M. 1975. Triplet state electron paramagnetic resonance studies of zinc porphyrins and zinc-substituted hemoglobins and myoglobins. *J. Am. Chem. Soc.* 97:1688–1694.

Horie, T. G. Maniara, and J. M. Vanderkooi. 1984. Interaction of electron acceptors with the excited triplet state of Zn cytochrome *c*. *FEBS Lett.* 177:287–290.

Jahn, H. A., and E. Teller. 1937. Stability of polyatomic molecules in degenerate electronic states I. Orbital degeneracy. *Proc. R. Soc. London Ser. A.* 161:220–225.

Kleibeuker, J. F., R. J. Platenkamp, and T. J. Schaafsma. 1978. The triplet state of photosynthetic pigments. I. Pheophytins. *Chem. Phys.* 27:51–64.

Kottis, P., and R. Lefebvre. 1963. Calculation of the electron spin resonance line shape of randomly oriented molecules in a triplet state. I. The $\Delta m = 2$ transition with a constant linewidth. *J. Chem. Phys.* 39:393–403.

Kottis, P., and R. Lefebvre. 1964. Calculation of the electron spin resonance line shape of randomly oriented molecules in a triplet state. II. Correlation of the spectrum with the zero field splittings. Introduction of an orientation-dependent linewidth. *J. Chem. Phys.* 41:379–393.

Krumhansl, J. A. 1986. Vibrational anomalies are not due to fractal geometry: comments on proteins. *Phys. Rev. Lett.* 56:2696–2699.

Langhoff, S. R., E. R. Davidson, M. Gouterman, W. R. Leenstra, and A. L. Kwiram. 1975. Zero field splitting of the triplet state of porphyrins.

J. Chem. Phys. 62:169–176.

Leenstra, W. R. 1979. Ph.D. dissertation. University of Washington, Seattle, WA.

Leeson, D. T., Berg, O., and Wiersma, D. A. 1994. Low-temperature protein dynamics studied by the long-lived stimulated photon echo. *J. Phys. Chem.* 98:3913–3916.

Levanon, H., and J. R. Norris. 1978. The photoexcited triplet state and photosynthesis. *Chem. Rev.* 78:185–198.

Levanon, H., A. Regev, T. Galili, M. Hugerat, C. K. Chang, and J. Fajer. 1993. Photoelectron transfer between a magnesium-free-base porphyrin heterodimer and duroquinone. Selective excitation and time-resolved EPR studies. *J. Chem. Phys.* 97:13198–13205.

Levanon, H., and A. Wolberg. 1974. Electron spin polarization in the photoexcited triplet state of porphyrins. *Chem. Phys. Lett.* 24:96–98.

Logovinsky, V., A. D. Kaposi, and J. M. Vanderkooi. 1993. Native and denatured Zn cytochrome c studied by fluorescence line narrowing spectroscopy. *Biochim. Biophys. Acta.* 1161:149–160.

Lhoste, J. M., C. Helene, and M. Ptak. 1967. Triplet states of biological interest *In* The Triplet State A. B. Zahlan, editor. Cambridge University Press, Cambridge. 479–503.

McGlynn, S. P., T. Azumi, and M. Kinoshita. 1969. Spectroscopy of the Triplet State. Prentice Hall, Englewood Cliffs, NJ. Chapter 5.

Meier, M., R. van Eldik, I-Jy Chang, G. A. Mines, D. S. Wuttke, J. R. Winkler, and H. B. Gray. 1994. Pressure effects on the rates of intramolecular electron transfer in ruthenium-modified cytochrome *c*. Role of the intervening medium in tuning distant Fe^{2+}:Ru^{3+} electronic couplings. *J. Am. Chem. Soc.* 116:1577–1578.

Pettigrew, G. W., and G. R. Moore. 1987. Cytochromes *c*. Biological Aspects. Springer-Verlag, Berlin.

Ponte Goncalves, A. M., and W. U. Spendel. 1977. Comments on the triplet state polarization in photosynthetic bacteria. *Chem. Phys. Lett.* 54:611–614.

Sarai, A. 1982. Dynamics of proton migration in free-base porphines. *J. Chem. Phys.* 76:5554–5563.

Schlicter, C. 1991. Principles of Magnetic Resonance, 3rd ed. Springer-Verlag, Berlin. 89–92.

Schwoerer, M., U. Konzelmann, and D. Klipper. 1972. Spin-phonon interactions for triplet state molecules in organic mixed crystals. *Chem. Phys. Lett.* 13:272–277.

Sims, L. J., T. M. Kite, and A. B. Dennison. 1972. Temperature-dependent saturation measurements in the photo-excited triplet state of pyrene-*d*-10. *J. Magn. Res.* 8:259–270.

Stevens, S. B., and H. J. Stapleton. 1990. Electron spin lattice relaxation in Yb^{3+}-doped silicate glasses. *Phys. Rev. B.* 42:9794–9801.

Suisalu, A., and R. Avarma. 1983. Phosphorescence-detected triplet state microwave resonance of a protoporphyrin molecule in *n*-octane. *Chem. Phys. Lett.* 101:182–186.

Thurnaurer, M. C., J. J. Katz, and J. R. Norris. 1975. The triplet state in bacterial photosynthesis: possible mechanisms of the primary act. *Proc. Natl. Acad. Sci. USA.* 72:3270–3274.

Turro, N. 1991. Modern Molecular Photochemistry. University Science Books, Mill Valley, CA. p. 190.

van der Est, A., R. Bittl, E. C. Abresch, W. Lubitz, and D. Stehlik. 1993. Transient EPR spectroscopy of perdeuterated Zn-substituted reaction centers of *Rhodobacter sphaeroides* R-26. 1993. *Chem. Phys. Lett.* 212: 561–568.

Vanderkooi, J. M., F. Adar, and M. Erecinska. 1976. Metallocytochrome *c*: characterization of electronic absorption and emission spectra of Sn and Zn cytochromes *c*. *Eur. J. Biochem.* 64:381–387.

Vanderkooi, J. M., and J. W. Berger. 1989. Excited triplet states to study biological macromolecules at room temperature. *Biochim. Biophys. Acta.* 976:1–27.

Vanderkooi, J. M., and M. Erecinska. 1975. Cytochrome *c* interaction with membranes. Absorption and emission spectra and binding characteristics of iron-free cytochrome *c*. *Eur. J. Biochem.* 60:199–207.

Vanderkooi, J. M., G. Maniara, T. J. Green, and D. F. Wilson. 1987. An optical method for the measurement of dioxygen concentration based upon quenching of phosphorescence. *J. Biol. Chem.* 262:5476–5482.

van der Waals, J. H., W. G. van Dorp, and T. J. Schaafsma. 1979. Electron spin resonance of porphyrin excited states. *In* The Porphyrins. D. Dolphin, editor. Academic Press, New York. 257–312.

van Noort, H. M., B. Wirnitzer, J. Schmidt, and J. H. van der Waals. 1982. The phosphorescent ^3E_u state of zinc porphin in *n*-alkane host crystals. *Mol. Phys.* 45:1259–1269.

Volker, S., and J. H. van der Waals. 1976. Laser-Induced photochemical isomerization of free-base porphyrin in an *n*-octane crystal at 4.2 K. *Mol. Phys.* 32:1703–1718.

Wagner, G. C., J. T. Colvin, J. P. Allen, and H. J. Stapleton. 1985. Fractal models of protein structure, dynamics and magnetic relaxation. *J. Am. Chem. Soc.* 107:5589–5594.

Wallin, S. A., E. D. A. Stemp, A. M. Everest, J. M. Nocek, T. L. Netzel, and B. M. Hoffman. 1991. Multiphase intracomplex electron transfer from cytochrome *c* to Zn cytochrome *c* peroxidase: conformational control of reactivity. *J. Am. Chem. Soc.* 113:1482–1484.

Wasserman, E., L. C. Snyder, and W. A. Yeager. 1964. ESR of triplet states of randomly oriented molecules. *J. Chem. Phys.* 41:1763–1772.

Walters, V., J. C. de Paula, G. T. Babcock, and G. E. Leroi. 1989. Resonance Raman spectrum of the lowest triplet state of Zn(II) tetraphenylporphyrin. *J. Am. Chem. Soc.* 111:8300–8302.

Weltner, W. 1983. Magnetic Atoms and Molecules. Dover Publications, New York. 156–218.

Zang, L., and A. H. Maki. 1990. Photoinduced electron transfer in the Zn-substituted cytochrome *c* $Ru(NH_3)_5$(His-33) derivative studied by phosphorescence and optically detected magnetic resonance. *J. Am. Chem. Soc.* 112:4346–4351.

Zhou, J. S., and N. M. Kostic. 1993a. Gating of photoinduced electron transfer from zinc cytochrome *c* and tin cytochrome *c* to plastocyanin. Effects of solution viscosity on rearrangement of the metalloprotein complex. *J. Am. Chem. Soc.* 115:10796–10804.

Zhou, J. S., and N. M. Kostic. 1993b. Comparison of electrostatic interactions and of protein–protein orientations in electron-transfer reactions of plastocyanin with the triplet state of zinc cytochrome and with zinc cytochrome *c* cation radical. *Biochemistry.* 32:4539–4546.

Zollfrank, J., J. Friedrich, J. M. Vanderkooi, and J. Fidy. 1991. Conformational relaxation of a low temperature protein as probed by photochemical hole burning: horseradish peroxidase. *Biophys. J.* 59:305–312.